Am J Cancer Res 2016;6(12):2772-2786
www.ajcr.us /ISSN:2156-6976/ajcr0044880

Original Article

PCAF acts as a gastric cancer suppressor through a novel PCAF-p16-CDK4 axis

Hong-Jun Fei[1*], Li-Dong Zu[1*], Jun Wu[1*], Xiao-Shu Jiang[2], Jing-Long Wang[1], Y Eugene Chin[3], Guo-Hui Fu[1]

[1]Pathology Center, Shanghai General Hospital/Faculty of Basic Medicine, School of Medicine, Shanghai Jiao Tong University, Shanghai 200025, P. R. China; [2]Department of Pathophysiology, Harbin Medical University, Harbin 150081, P. R. China; [3]Institute of Health Sciences, Shanghai Institutes of Biological Sciences, Chinese Academy of Sciences, Shanghai, P. R. China. [*]Equal contributors.

Received November 22, 2016; Accepted November 29, 2016; Epub December 1, 2016; Published December 15, 2016

Abstract: Gastric cancer (GC) is a leading cause of cancer-related death worldwide and the pathogenesis of GC remains largely unknown. Here, we demonstrate a novel mechanism by which P300/CBP associating factor (PCAF) acts as a tumor suppressor in GC cells. We showed that both PCAF mRNA and protein were downregulated in GC cells, and that this downregulation correlated with poor survival. Meanwhile, the interaction between human anion exchanger 1 (AE1) and p16 is a key event in GC development. We found that PCAF inhibited GC growth by interacting with AE1 and p16 to promote ubiquitin-mediated degradation of AE1 and p16 upregulation and translocation into the nucleus. Binding of nuclear p16 to CDK4 prevented the CDK4-Cyclin D1 interaction to inhibit GC proliferation. Furthermore, reduced PCAF levels in GC cells were associated with intracellular alkalinization and decreased immunity. Together these results suggest that PCAF acts as a GC suppressor through a novel PCAF-p16-CDK4 axis. The downregulation of PCAF expression in GC cells that follows intracellular alkalinization and decreased immune response, indicates that GC therapies should focus on restoring PCAF levels.

Keywords: GC, PCAF-P16-CDK4 axis, AE1, proliferation

Introduction

Gastric cancer (GC) is the second leading cause of cancer mortality worldwide [1]. Although remarkable progress has been made in surgical and clinical therapies for GC, including targeted therapy [2-4] and immunotherapy [5], the prognosis of GC, especially poorly differentiated gastric cancer (PGC), remains poor. Moreover, excess cell proliferation in GC patients makes this type of cancer challenging to treat. Whether genetic and epigenetic mechanisms are involved in GC progression is unclear, and thus the molecular mechanisms responsible for GC cell proliferation require further characterization.

P300/CBP associating factor (PCAF) is a histone acetyltransferase (HAT) that acetylates mainly H3 histones and has a strong link with tumor initiation and progression [6-8]. PCAF is also involved multiple biological and pathogenic processes such as proliferation, differentiation, and apoptosis [9-11], because of its ability to acetylate non-histone proteins including Smad [12], c-myc [13], and p53 [14]. Increasing evidence indicates that PCAF is not only a HAT, but also acts as an ubiquitination factor through its intrinsic E3 ligase activity, which promotes ubiquitin-dependent protein degradation [15, 16]. Intriguingly, several studies reported that the dual functionality of PCAF is important in different types of cancer. Indeed, PCAF has cancer-promoting activity in lung adenocarcinoma [17] and brain cancer [18], but appears to have an antitumor function in hepatocellular cancer [19].

Numerous studies have shown that p16 is a negative regulator of cell cycle progression [20, 21]. p16 inhibition of CDK4 and CDK6 regulates the transition between the G1- to S-phases of the cell cycle and eventually suppresses cell proliferation [22, 23]. In different tumor types in humans, the p16 gene shows homozygous deletion, mutations, or methylation that inhibits

its transcription [24]. Notably, p16 shows cytoplasmic expression in GC [25, 26] and oropharyngeal cancer [27], and this localization can serve as a prognostic marker. In humans the underlying mechanism by which p16 mislocalizes to the cytoplasm involves human anion exchanger 1 (AE1) [28]. AE1 expression is normally restricted to red blood cell (RBC) membranes where it mediates Cl-/HCO3- exchange across the plasma membrane to regulate intracellular pH (pHi) [29]. However, in GC cells AE1 showed an unexpected cytoplasmic localization indicating that it failed to traffic to the plasma membrane. This cytoplasmic localization allows p16 and AE1 to interact, resulting in the sequestration of p16 in the cytoplasm. This interaction is associated with intracellular alkalinization and cell cycle promotion, suggesting that AE1 can act as an onco-protein in GC cells.

Here we found that PCAF expression was aberrantly downregulated in GC tissues. Furthermore, both *in vitro* and *in vivo* assays showed that PCAF inhibited GC growth by promoting ubiquitin-mediated degradation of AE1. Together these results indicate a potential regulatory axis composed of PCAF-p16-CDK4, and that acidic stimuli or IFN-γ treatment could have beneficial effects in GC.

Materials and methods

GC tissue microarray

GC tissue microarrays (TMAs) including 210 GC specimens were prepared in our lab. For TMA construction, duplicate 1.0 mm diameter cores of tissue from each sample were punched from paraffin tumor blocks and corresponding non-tumor tissues in the training cohort or from cores of primary tumor biopsies in the validation cohorts. As a tissue control, the biopsies of normal gastric epithelium tissues were inserted in the four corners and the center of each slide.

Cell culture, reagents and transfections

The WGC cell line MKN28, PGC cell lines SGC7901, AGS and MKN45 and human gastric mucosal epithelial cell line GES-1 were cultured in RPMI-1640 (Hyclone, Logan, UT, USA) containing 10% fetal bovine serum (FBS, Hyclone) and 1% penicillin/streptomycin (Invitrogen, Carlsbad, CA, USA) in an atmosphere of 5% CO_2 at 37°C. In some experiments the proteasome inhibitors cycloheximide (CHX, Sigma-Aldrich, St. Louis, MO, USA, 25 μg/ml) or MG132 (10 mM, Merck KgaA Darmstadt, Germany) were added to the culture medium.

Antibody information

Antibodies used for western blot or IP experiments were: anti-PCAF (Cell Signaling Technology (CST)), anti-p16 (BD Pharmingen, Le Pont de Claix, France), anti-GFP (Santa Cruz), anti-HA (Santa Cruz), anti-β-actin (Sigma-Aldrich), anti-AE1 (Abcam, MA, USA), anti-Vinculin (Abcam, MA, USA), anti-Lamin B (Santa Cruz), anti-Flag (Sigma-Aldrich) and anti-CDK4 (CST). Transfection of GC cells was performed with Lipofectamine 2000 (Invitrogen, CA, USA) or X-treme (Roche) according to the manufacturer's instructions.

Immunohistochemistry

Immunohistochemistry was performed on 4 μm sections of formalin fixed, paraffin embedded tumors, which were cut and placed on clean microscopic slides. The sections were dewaxed in xylene, rehydrated in graded alcohol, and rinsed in water. Antigen retrieval of the tissues was then performed at 100°C for 20 min with 10 mM citrate buffer, pH 6. A peroxidase block reagent was applied on the specimen according to the tissue size and incubated for 5-10 min at room temperature. Primary PCAF antibody (Santa Cruz) was applied at 1:100 dilution and p16 antibody was applied at 1:200 dilution. Staining development was achieved by incubation with DAB (MaiXin, China). The slides were then viewed and analyzed under a light microscope.

Clinical data set analysis

For survival analyses, overall survival stratified by expression of the gene of interest was presented as Kaplan-Meier plots and tested for significance using log-rank tests. The analysis was performed according to the manufacturer's instructions (http://kmplot.com/analysis/index.php?p) [30].

Western blot and immunoprecipitation

For western blot, cells were lysed at 4°C for 10 min in lysis buffer (100 mM Tris-HCl (pH 7.0), 4% SDS, 20% glycerol, 200 mM DTT) with a 1% protease inhibitor cocktail and 1 mM phenyl-

methylsulfonyl fluoride (PMSF, Roche Science). After boiling for 5 min at 95°C three times, the lysates were centrifuged at 12,000 rpm for 15 min at 4°C. The resulting supernatants were resolved by SDS-PAGE and transferred to nitrocellulose membranes. To block the membranes, 10% skim milk in TBST was used to reduce nonspecific background. Then, the membranes were incubated overnight at 4°C with primary antibodies. After washing with TBST three times, the membranes were incubated for 1 h at room temperature with HRP-conjugated secondary antibodies (Jackson), and then washed. Bound antibodies were detected by chemiluminescence (Pierce, Rockford, IL, USA).

For immunoprecipitation (IP), 3×10^7 cells were lysed with lysis buffer containing 50 mM Tris-HCl (pH 7.4), 150 mM NaCl, 1% Nonidet P-40 (NP-40), 1 mM EDTA and protease inhibitor for 60 min at 4°C. Lysates were pre-cleared with protein A/G agarose beads. The supernatants were immunoprecipitated with specific antibodies overnight at 4°C. Then, protein A/G agarose beads were added and samples were incubated for 45 min at 4°C. After three washes with RIPA buffer, immunocomplexes were analyzed by immunoblotting. The IP was done with PCAF (CST), Flag M2 affinity Gel (Sigma), p16 (BD Pharmingen) and GFP (Santa Cruz).

Quantitative real-time PCR analysis

Total RNA in GC cells was extracted using TRIzol (Invitrogen) after the cells were cultured at pH 6.0, 6.5 and 7.0 for 24 and 48 hours, respectively. The cDNA was reverse-transcribed from 1 mg total RNA using a reverse transcriptase kit (Toyobo). Q-PCR was performed using a 7500 Real-Time PCR System (Applied Biosystems) and SYBR Green PCR Master Mix (BioRad). GAPDH was used for normalization. Primer sequences used were: AE1 5'-CCGCTTCATCTCCCGCTAT-3'; 5'-TTGGGCACCATCAACACG-3'; GAPDH 5'- CTCCTCCTGTTCGACAGTCAGC-3'; 5'-CCCAATACGACCAAATCCGTT-3'; PCAF 5'-AACGCAGGGAGCAGCAGT-3'; 5'-CAGGGTCCGTGATGGTAG-3'.

Cell proliferation assays and cell cycle analysis

GC cells were transfected with empty vector or PCAF constructs and then counted and seeded in 6 well-plates. For cell proliferation, the number of cells was quantified at different times after transfection. For cell cycle analysis, GC cells were harvested, washed in PBS, and then fixed with 70% cold ethanol. Finally, cells were incubated with 50 μg/mL propidium iodide (PI) solution and 200 mg/ml RNase for 30 min at room temperature. DNA contents were analyzed using flow cytometry.

Cell fractionation

For nuclear and cytoplasmic fractionations, 1×10^7 cells were washed twice with cold phosphate-buffered saline (PBS), then incubated in 1 ml lysis buffer (10 mM HEPES, 1.5 mM $MgCl_2$, 10 mM KCl, 0.5 mM DTT, pH 7.9) on ice for 10 min. After adding NP-40 to a final concentration of 0.2%, lysates were vortexed and centrifuged at 12,000 rpm for 20 min to collect the supernatants (post-nuclear fraction) as "cytoplasmic protein". The pellets containing the nuclear fraction were washed with lysis buffer without NP-40 and resuspended in 150 μL extraction buffer, and incubated for 20 min on ice. SDS lysis buffer (150 μL) was added to the nuclear proteins.

Immunofluorescence analysis

SGC7901 cells were transfected with empty vectors or PCAF constructs and grown on coverslips. After 48 hours, the cells were fixed in 4% paraformaldehyde for 15 min at room temperature. The cells were washed in PBS three times and then incubated with anti-PCAF and anti-p16 antibodies overnight at 4°C. Alexa Fluor 488-conjugated goat anti-rabbit antibody and Alexa Fluor 594-conjugated goat anti-mouse antibody (Invitrogen) were used as the secondary antibodies. The coverslips were photographed under a confocal microscope.

Ubiquitination assay

SGC7901 cells were transfected with empty vector or PCAF, HA-tagged ubiquitin, or Flag-tagged AE1 constructs for 24 hours, and then treated with 10 μM MG132 for an additional 6 hours. Cell extracts were incubated with Flag M2 affinity gel for 5 hours at 4°C. The proteins were separated from the beads and resolved by 10% SDS-PAGE gels, then analyzed by western blot with anti-HA antibody.

Statistical analysis

All data represent at least three independent experiments and are expressed as means and

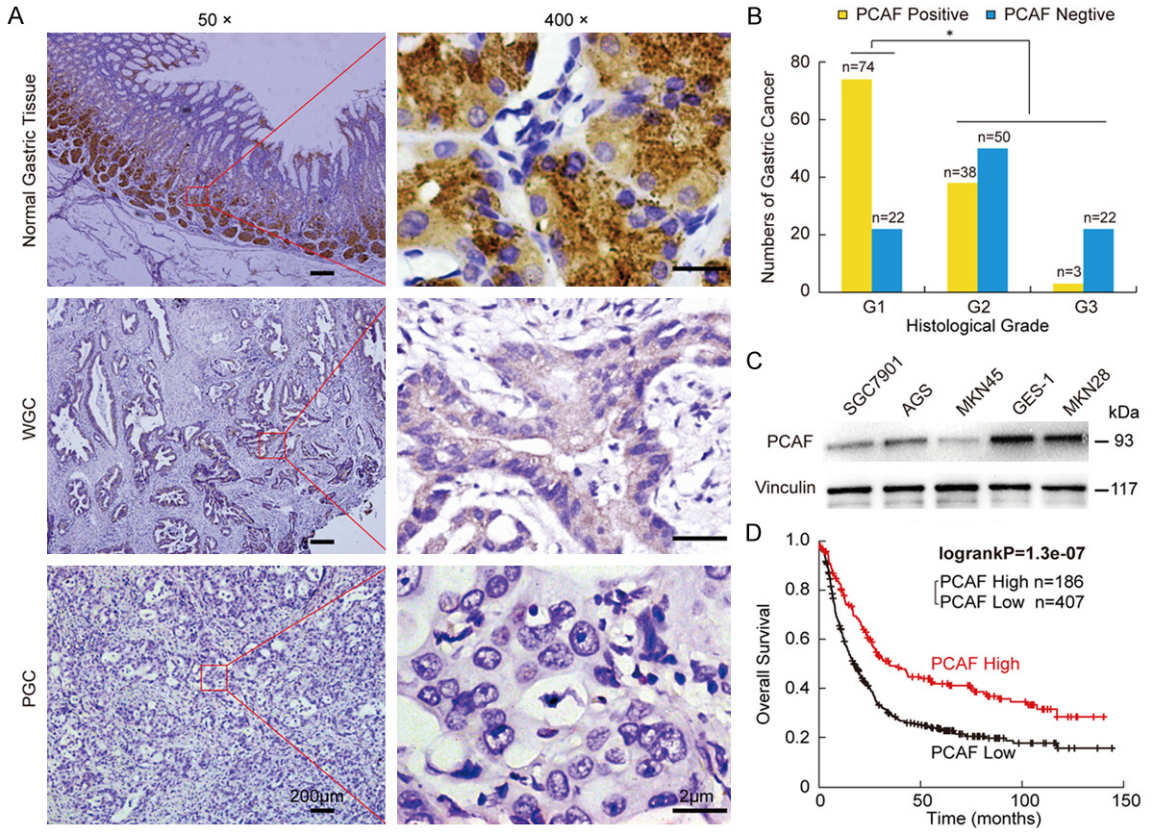

Figure 1. PCAF is downregulated in GC cells and loss of PCAF is correlated with poor differentiation and survival. A: Immunohistochemistry (IHC) of PCAF in non-cancer, WGC, and PGC tissues. B: Statistical analysis of the correlation between PCAF expression and clinical stage of GC patients. C: Western blot analysis of PCAF expression in GC cells as indicated. D: Kaplan-Meier plots of overall survival of GC patients, stratified by PCAF expression. Data were obtained from the Kaplan-Meier plotter public database. The *p* value was calculated by a log rank test.

standard errors of the mean. Determination of the significance of differences among groups was assessed using the Student's t-test. P< 0.05 was considered statistically significant. The log-rank test was used to generate *p* values of Kaplan-Meier survival analyses. Demographic information of patients from the low PCAF and high PCAF groups was compared by χ^2 test.

Results

Loss of PCAF function is associated with poor prognosis of GC patients

To explore the role of PCAF in GC development, PCAF expression in 210 tissue samples, 4 GC cell lines, and 1 human gastric mucosal epithelial cell line was detected by immunohistochemistry (IHC) or western blot. Lower PCAF expression levels correlated with poor differentiation (**Figure 1A**; Supplementary Table 1) and higher GC grade (**Figure 1B**). These results were consistent with those found in GC cell lines (**Figure 1C**). Notably, GC patients with lower PCAF expression levels had markedly reduced survival times relative to patients with high PCAF expression levels (**Figure 1D**). Taken together, these findings indicate that impaired PCAF expression might be associated with GC development.

PCAF impaired the interaction between AE1 and p16 by interacting with and promoting degradation of AE1

We previously explored the direct interaction of AE1 and p16 in the cytoplasm, which is a key event in GC progression, and how targeting AE1 could significantly inhibit GC growth *in vitro* and *in vivo* [28, 31-34]. We therefore hypothesized that PCAF could block AE1 and p16 interactions. To test this possibility, PCAF expression constructs were transfected into SGC7901 cells either alone or with AE1 expression con-

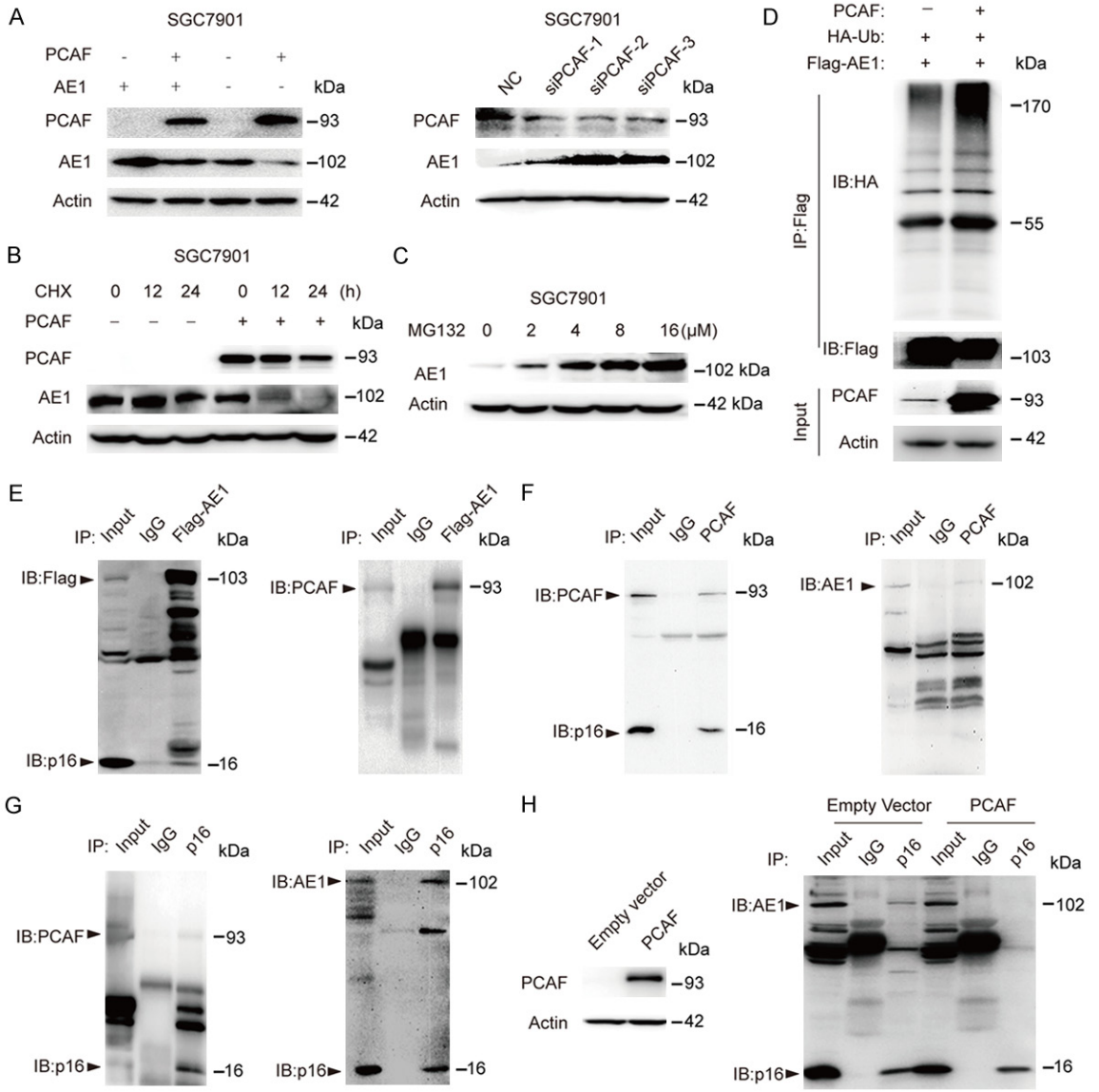

Figure 2. PCAF impaired the interaction of AE1 and p16 by interacting with AE1 and promoting its degradation. Western blot showing: A: AE1 expression was downregulated in SGC7901 cells that overexpress PCAF (left) and was upregulated in cells transfected with PCAF-targeting siRNAs (right); B: AE1 protein was rapidly degraded in SGC7901 cells. Cells with or without PCAF transfection were treated with cycloheximide (CHX, 25 μg/ml) for the indicated time; C: AE1 expression in SGC7901 cells either treated or not with MG132 at different concentrations; D: Ubiquitination assay wherein AE1 and ubiquitin expression constructs were co-transfected with or without PCAF into SGC7901 cells, and AE1 ubiquitination was determined. Immunoprecipitation assay showed that: E: p16 (left) and PCAF (right) were pulled down by anti-Flag (AE1) antibody in SGC7901 cells, whereas AE1 was determined by anti-Flag antibody. Cells were transfected with AE1 expression constructs for 48 hours; F: Endogenous p16 (left) and AE1 (right) were pulled down by anti-PCAF antibody in SGC7901 cells; G: Endogenous PCAF (left) and AE1 (right) were pulled down by anti-p16 antibody in SGC7901 cells; H: SGC7901 cells were transfected with or without PCAF expression constructs for 48 hours. Whole cell lysates were immunoprecipitated by anti-p16 antibody and AE1 was detected by western blot.

structs and AE1 expression in the cells was detected. Western blots showed that overexpressed PCAF decreased both endogenous and exogenous expression of AE1, whereas PCAF knockdown increased expression of endogenous AE1 (**Figure 2A**). These results suggested that PCAF affected AE1 expression by stabilizing the AE1 protein. To this end, SGC-

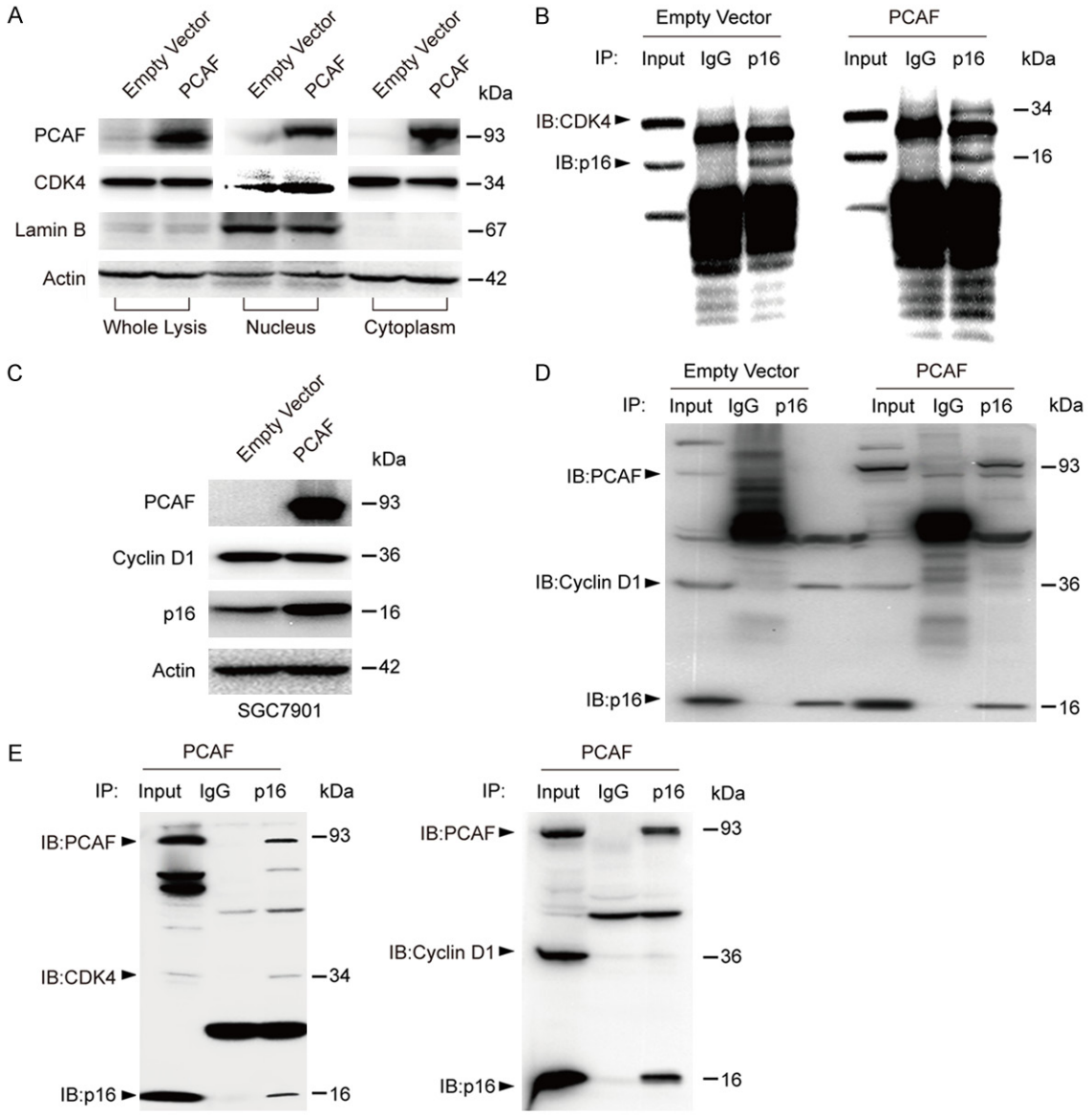

Figure 3. p16 competes with CDK4 for Cyclin D1 binding. A: PCAF promoted CDK4 translocation into nuclei of SGC7901 cells transfected with PCAF expression constructs for 48 hours. The cells were fractionated into nuclear and cytoplasmic fractions and CDK4 expression was detected by western blot. B: SGC7901 cells were transfected with PCAF expression constructs or empty vectors for 48 hours. Whole cell lysates were immunoprecipitated by anti-p16 antibody and CDK4 and detected by western blot. C: PCAF does not affect Cyclin D1 expression in SGC7901 cells transfected with PCAF expression constructs or empty vectors for 48 hours. D: PCAF impaired the interaction between Cyclin D1 and p16 in SGC7901 cells transfected with PCAF expression constructs or empty vectors for 48 hours. Whole cell lysates were immunoprecipitated with anti-p16 antibody and Cyclin D1 was detected by western blot. E: PCAF promoted the interaction of p16 and CDK4 by sequestering Cyclin D1 in SGC7901 cells. Cells were transfected with or without PCAF expression constructs for 48 hours and whole cell lysates were immunoprecipitated by anti-p16 antibody. PCAF, p16, CDK4 and Cyclin D1 expression was detected by western blot.

7901 cells were treated with cycloheximide (CHX) for different times to inhibit protein synthesis. Compared with the control cells, AE1 was rapidly degraded in cells transfected with PCAF expression constructs following inhibition of protein synthesis (**Figure 2B**).

A study by Patterson and Reithmeier reported that ectopically expressed AE1 was degraded through the ubiquitin proteasome pathway [35]. As such, we hypothesized that PCAF could decrease AE1 expression by promoting its ubiquitination and subsequent proteasomal degra-

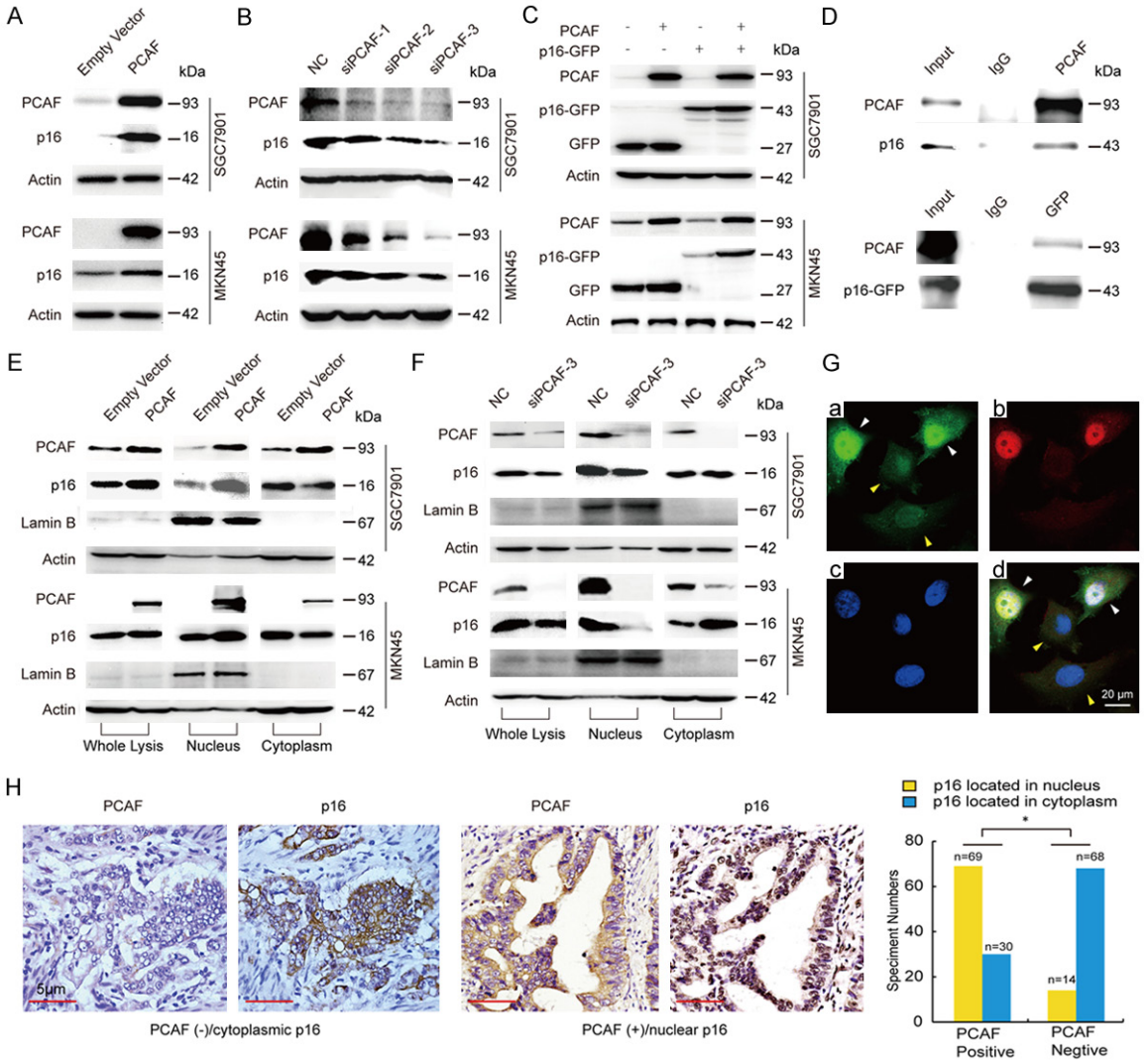

Figure 4. PCAF up-regulates p16 expression and promotes its nuclear localization. Western blot showing that: A: p16 expression was increased in SGC7901 and MKN45 cells with overexpressed PCAF; B: p16 expression was decreased in SGC7901 and MKN45 cells transfected with PCAF-targeted siRNAs; C: PCAF up-regulated GFP-p16 expression in both SGC7901 and MKN45 cells. D: SGC7901 cells were transfected with PCAF and GFP-p16 expression constructs and the interaction was detected by co-immunoprecipitation. E: PCAF promoted the translocation of p16 into the nucleus in both SGC7901 (top) and MKN45 (bottom) cells transfected with PCAF expression constructs for 48 hours. The cells were fractionated into nuclear and cytoplasmic fractions and p16 expression was detected by western blot. F: PCAF knockdown impaired p16 translocation into the nucleus in both SGC7901 (top) and MKN45 (bottom) cells transfected with PCAF-targeting siRNAs for 48 hours. The cells were fractionated into nuclear and cytoplasmic fractions and p16 expression was detected by western blot. G: Immunofluorescence showing that more p16 had a nuclear localization (green) in the presence of PCAF (red): a, p16 staining; b, PCAF staining; c, DAPI staining; d, merge of a, b and c profiles. White arrows indicate cells transfected with PCAF constructs and yellow arrows indicate cells without PCAF transfection; H: PCAF and p16 staining of serial GC tissue sections (left). Statistical analysis showing that PCAF levels correlated with nuclear p16 (right). *P<0.05.

dation. Western blotting of SGC7901 cells treated with the proteasome inhibitor MG132 at different concentrations showed a dose-dependent accumulation of AE1 (**Figure 2C**). Furthermore, ubiquitin-mediated degradation of AE1 was promoted by PCAF (**Figure 2D**). Taken together, these results suggested that PCAF-AE1 interactions might promote AE1 degradation by the proteasome, and that the p16-AE1 interaction could be impaired in the presence of PCAF. To test this possibility, PCAF, Flag-AE1, and p16 expression constructs were

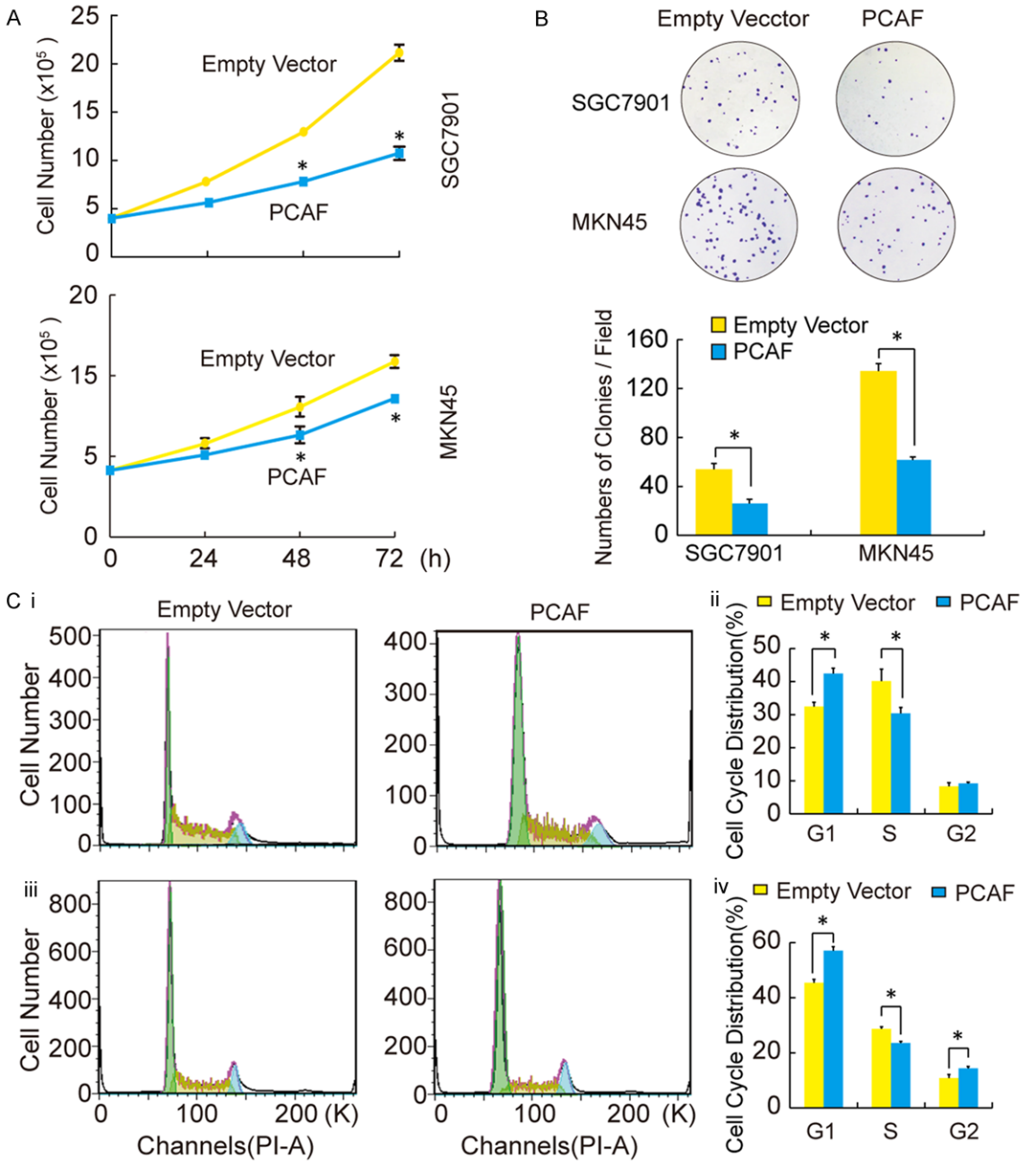

Figure 5. PCAF overexpression inhibited GC cell proliferation. (A) SGC7901 (top panel) and MKN45 (bottom panel) cells were transfected with PCAF expression constructs or empty vector for the indicated times before cell numbers were counted *P<0.05. (B) SGC7901 and MKN45 cells were transfected with PCAF expression constructs or empty vector for 48 hours and the cells were then seeded in 6-well plates and cultured for 7 days before the resulting colonies (top panel) were counted (bottom panel) and (C) flow cytometry was performed: (i) FACS analysis of cells transfected with empty vector (left) or PCAF expression constructs (right); (ii) Statistical analysis for (i); (iii) and (iv) The experimental design was the same as for (i) and (ii). *P<0.05. Three independent experiments were performed for the above assays.

co-transfected into SGC7901 cells for 48 hours and the interaction of the three proteins was assessed by immunoprecipitation (IP). The results indicated that PCAF and p16 could be simultaneously pulled down by an anti-Flag antibody (**Figure 2E**). Furthermore, endogenous AE1 and p16 could be simultaneously pulled down by an anti-PCAF antibody (**Figure 2F**) or anti-p16 antibody (**Figure 2G**), whereas PCAF overexpression impaired the interaction bet-

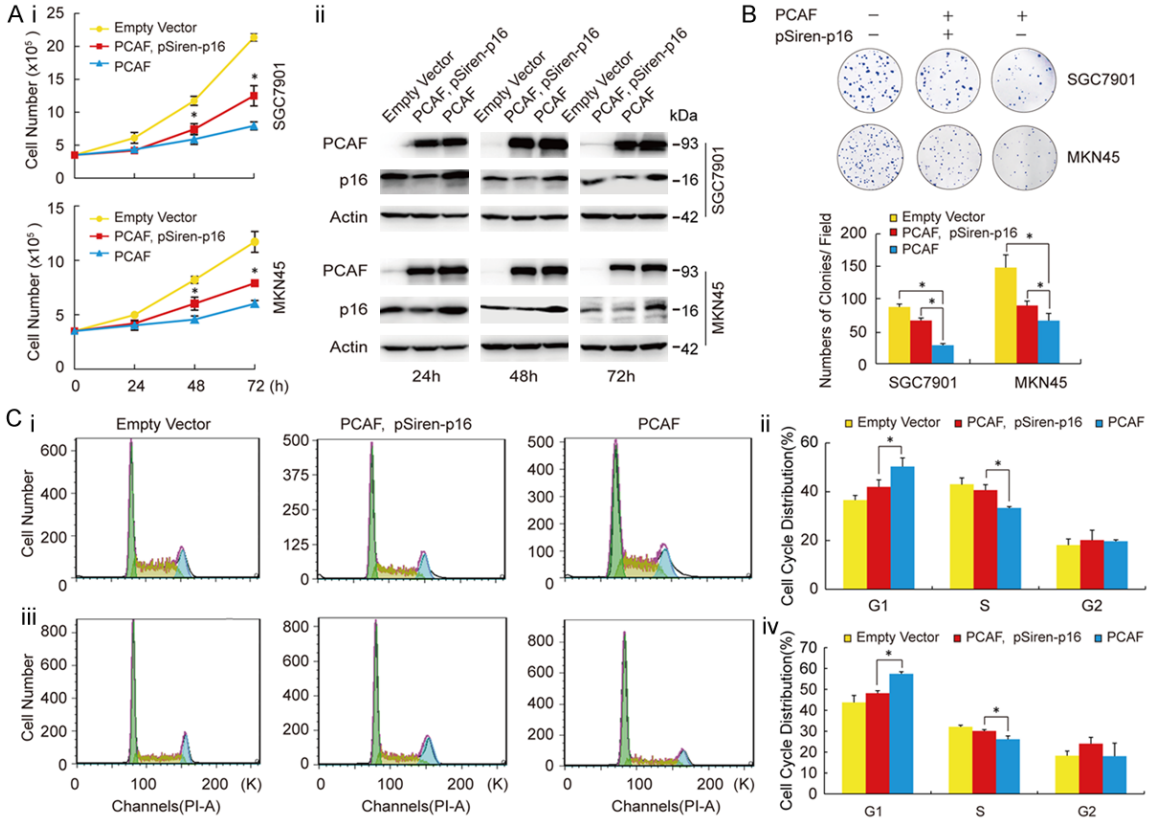

Figure 6. p16 knockdown impaired the PCAF-mediated inhibition of GC cell proliferation. (A) SGC7901 (top) and MKN45 (bottom) cells were (i) co-transfected with p16-targeting siRNAs and PCAF expression constructs or with PCAF transfection or empty vector alone for the indicated times before the cell numbers were counted. *P<0.05; (ii) Western blot showing PCAF and p16 expression in the same cells with the indicated transfection conditions; (B) SGC7901 and MKN45 cells were transfected with PCAF expression constructs or co-transfected with p16-targeting siRNAs or empty vector alone for 48 hours before the cells were seeded on 6-well plates and cultured for 7 days. The resulting colonies are shown (top panel) and the colony number was counted (bottom panel). *P<0.05. (C) SGC7901 (top line) or MKN45 (bottom line) cells were transfected with PCAF expression constructs or co-transfected with p16-targeting siRNAs or empty vector alone for 48 hours and the cell cycle stage was detected by flow cytometry: (i) FACS analysis in cells transfected with empty vector (left), PCAF expression constructs and p16-targeting siRNAs (middle) or PCAF expression constructs (right); (ii) Statistical analysis of (i); (iii) and (iv) The experimental design was the same as (i) and (ii). *P<0.05. Three independent experiments were performed for each of the above assays.

ween AE1 and p16 (**Figure 2H**). These results indicate that the activities of PCAF, AE1, and p16 are closely correlated.

PCAF promoted an interaction between p16 and CDK4 and impaired the interaction of CDK4 with Cyclin D1

Given that p16 and Cyclin D1 are known to competitively interact with CDK4, we next evaluated the effect of PCAF on the p16-CDK4 interaction or the interaction between CDK4 and Cyclin D1. PCAF overexpression did not affect CDK4 expression, but instead facilitated its nuclear localization and interaction with p16 (**Figure 3A**, **3B**). On the other hand, Cyclin D1 expression was not affected by overexpressed PCAF, although the interaction between CDK4 and Cyclin D1 was impaired (**Figure 3C**, **3D**). Furthermore, an anti-p16 antibody pulled down PCAF and CDK4 but not Cyclin D1 in cells that overexpressed PCAF (**Figure 3E**).

PCAF upregulated p16 expression and promoted nuclear translocation of p16

We previously found that p16 was ectopically expressed in the cytoplasm of GC cells and was involved in GC progression. To address whether reductions in PCAF levels are associated with the cytoplasmic expression of p16, we explored the relationship between PCAF and p16. Enforced expression of PCAF in SGC7901 and MKN45 PGC cells upregulated p16 expression

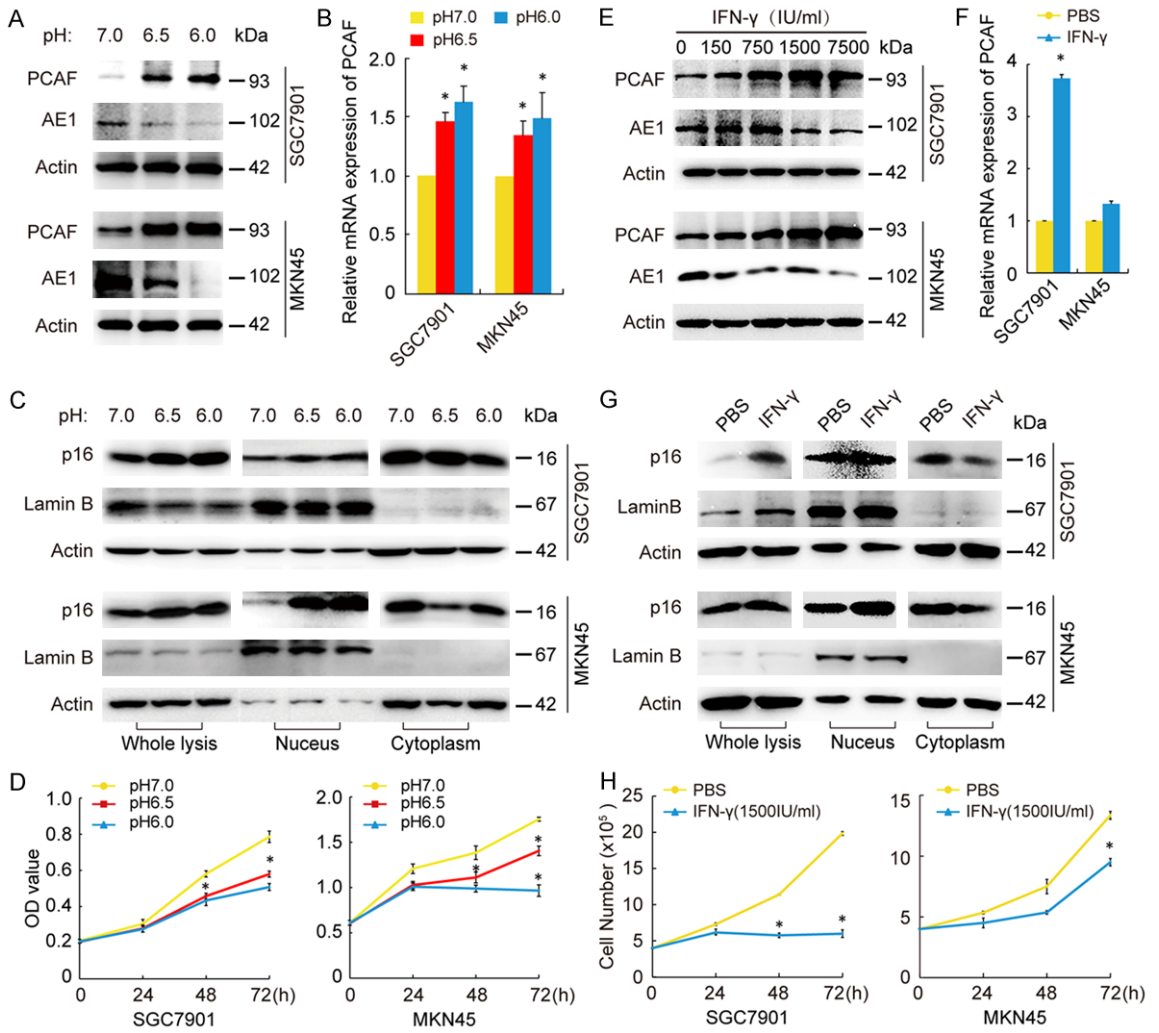

Figure 7. Upregulation of PCAF expression in cells cultured with lower pH or IFN-γ. (A) Western blot showing that PCAF expression was upregulated whereas AE1 was downregulated in SGC7901 (top) and MKN45 (bottom) cells exposed to low pH. Cells were cultured at the indicated pH for 48 hours; (B) Q-PCR determination of PCAF and AE1 mRNA levels in SGC7901 and MKN45 cells. Cells were treated the same as in (A); (C) p16 nuclear translocation was promoted in SGC7901 (top) and MKN45 (bottom) cells after treatment with lower pH for 48 hours. The cells were fractionated into nuclear and cytoplasmic fractions and p16 expression was detected by western blot. (D) GC cell proliferation was inhibited under acidic culture conditions. (E) Western blot showing that PCAF and AE1 expression levels were upregulated and downregulated, respectively, in SGC7901 (top) and MKN45 (bottom) cells following treatment with IFN-γ for 48 hours. (F) Q-PCR detection of PCAF and AE1 mRNA levels in SGC7901 and MKN45 cells. Cells were treated the same as in (E). (G) The translocation of p16 into the nucleus was promoted in SGC7901 (top) and MKN45 (bottom) cells following treatment with IFN-γ for 48 hours. The cells were fractionated into nuclear and cytoplasmic fractions and p16 expression was detected by western blot. (H) GC cell proliferation was inhibited by treatment with IFN-γ.

(**Figure 4A**). Conversely, p16 protein levels were reduced when PCAF-targeted siRNAs were transfected into the same cells (**Figure 4B**). Furthermore, when GFP-p16 expression constructs were co-transfected into SGC7901 and MKN45 cells with PCAF expression constructs, the GFP-p16 protein level was upregulated in PCAF-overexpressing cells relative to cells transfected with empty vector (**Figure 4C**). However, the p16 mRNA levels were not changed by PCAF expression (data not shown). These results indicated that PCAF regulates p16 at the protein level.

Next, we used co-IP to test whether interactions with PCAF stabilize the p16 protein. PCAF and p16 could indeed be pulled down by antibodies specific to each protein (**Figure 4D**). In

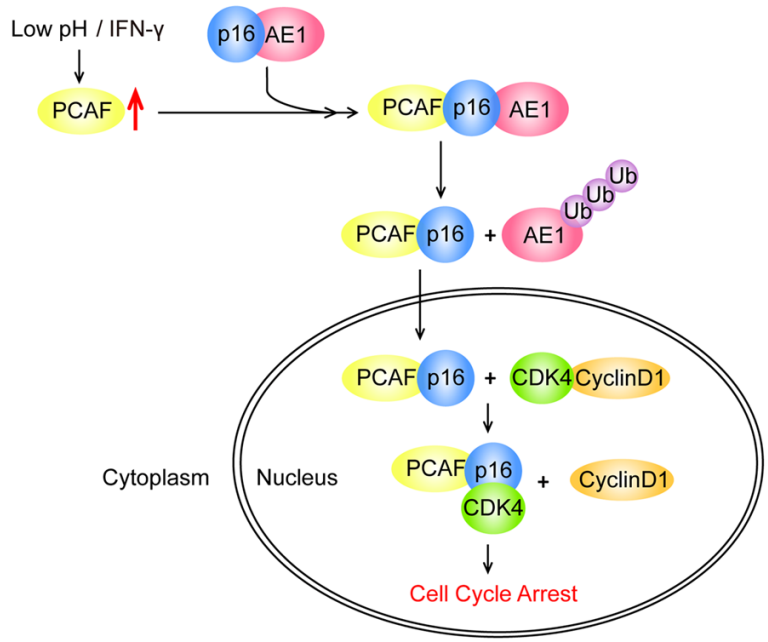

Figure 8. A proposed working model for PCAF-mediated ubiquitination of AE1 that connects to the PCAF-p16-CDK4 pathway in GC cells. In the presence of lower pH or IFN-γ stimuli, PCAF expression in GC cells is upregulated. This elevation in PCAF levels promotes an AE1-PCAF interaction and ubiquitin-mediated degradation of AE1. Meanwhile, PCAF could also interact with p16 to upregulate its expression, and promote p16 nuclear translocation. Once in the nucleus, p16 can compete with Cyclin D1 for binding to CDK4, which leads to cell cycle arrest and inhibition of GC proliferation.

addition, forced expression of PCAF increased p16 expression and enhanced its nuclear translocation (**Figure 4E**). In contrast, PCAF knockdown in SGC7901 and MKN45 cells led to PCAF downregulation and increased amounts of p16 in the cytoplasm (**Figure 4F**). Immunofluorescence experiments further confirmed a higher amount of nuclear staining of p16 in cells with PCAF overexpression (**Figure 4G**). IHC of 181 serial sections from GC specimens showed a significant correlation between PCAF expression and p16 distribution, namely that nuclear distribution of p16 was observed in PCAF-positive tissues, whereas a cytoplasmic distribution of p16 was seen in PCAF-negative tissues (**Figure 4H**).

PCAF overexpression inhibited proliferation and colony formation by PGC cells

The results presented here suggest that a novel PCAF-p16-CDK4 axis might be involved in inhibiting GC proliferation. To test this possibility, pCDNA3-PCAF constructs were transfected into PGC SGC7901 and MKN45 cells and cell proliferation was determined. When both GC cell lines overexpressed PCAF, cell growth and colony formation were inhibited compared with the control cells (**Figure 5A**, **5B**). Furthermore, flow cytometry analysis showed that PCAF increased the percentage of GC cells in the G1/S stage of the cell cycle (**Figure 5C**). Taken together, these results indicated that PCAF inhibits GC proliferation by inducing cell cycle arrest.

Knockdown of p16 blocked PCAF-mediated inhibition of GC proliferation

In light of the correlation between PCAF and p16, we asked whether p16 is crucially involved in PCAF-mediated GC suppression. We co-transfected pCDNA3-PCAF and pSiren-p16 into SGC7901 and MKN45 cells, and then determined cell counts and colony numbers. Cells co-transfected with PCAF and pSiren-p16 grew faster than cells with PCAF transfection alone (**Figure 6A**, **6B**). Moreover, p16 knockdown increased the ratio of cells in the G1/S stage (**Figure 6C**). These results demonstrated that p16 is important for PCAF-mediated GC inhibition.

PCAF levels were upregulated by acidic culture or IFN-γ treatment

To explore the underlying mechanism of PCAF loss in GC cells, we sequenced whole genomic DNA, including the PCAF gene, extracted from SGC7901 and MKN28 cells and found no mutations (data not shown). Since intracellular alkalinization appears to occur in GC cells [33], we cultured SGC7901 and MKN45 cells in acidic (Ph 6.0-7.0) conditions for 48 hours and then assessed PCAF expression by western blot. The PCAF mRNA and protein expression level of PCAF in the two GC cell lines both gradually increased with culture at lower pH conditions (**Figure 7A**, **7B**). Meanwhile, we also observed downregulation of AE1 expression as well as upregulation and nuclear translocation of p16

protein (**Figure 7C**). The AE1 and p16 mRNA levels remained unchanged (**Figure 7B** and data not shown, respectively). Moreover, in response to increased PCAF levels induced following culture in acidic media, GC cell growth was inhibited (**Figure 7D**).

We also examined the effect of IFN-γ on PCAF levels. As with acidic stimulation, IFN-γ treatment enhanced the expression of PCAF mRNA and protein (**Figure 7E**, **7F**), which in turn reduced AE1 levels and nuclear translocation of p16 (**Figure 7G**). Similar to acid treatment, INF-γ inhibited GC cell proliferation by upregulating PCAF (**Figure 7H**). Based on these results, we propose a novel mechanism by which PCAF can mediate GC suppression (**Figure 8**).

Discussion

Cancers in different organs can have different molecular characteristics and the same molecules in different types of tumors may have opposite functions. In this study, we provide direct evidence and show for the first time that the histone deacetylase PCAF is critically required for negative regulation of cell cycle progression that plays a key role in GC inhibition. In contrast to PCAF in lung and brain cancers, low expression levels of PCAF in GC tissues are correlated with adverse clinicopathologic features and strongly suggest that PCAF functions as a GC suppressor. Our data presented here demonstrated that PCAF inhibited GC growth by downregulating AE1 levels and upregulating p16 via direct interaction. The interaction between AE1 and p16 was first identified through yeast two hybridization screening and confirmed by pull-down and immunoprecipitation assay [28, 36]. Moreover, the role of this interaction in GC development was documented both *in vitro* and *in vivo* [32]. First, PCAF promotes degradation of AE1 by the ubiquitin proteasome system that in turn interrupts the interaction between AE1 and p16 and increases the likelihood of p16 binding to PCAF. These results are consistent with our previous finding that GC patients with high AE1 expression had poorer overall survival time than those with low AE1 expression. Moreover, in animal experiments, mice treated with AE1-targeted siRNA had tumor incidences that decreased significantly from 68%-72% in the untreated control group to 15.8% in the siRNA treatment group [32, 37]. Second, the PCAF and p16 complex can recruit CDK4 away from interactions with Cyclin D1, which subsequently inhibits cell proliferation.

Dysregulation of PCAF expression has been reported in various solid tumors, including colon, lung, and hepatocellular cancer, thus indicating a strong link between PCAF tumor initiation and progression [17, 38, 39]. Changes in the GC tumor microenvironment could be an essential cue to reduce PCAF levels during GC progression. Accumulating data confirmed that many immune system cytokines, such as CKCL8 [40], IL-8 [41], and IFN-γ [42], were associated with GC development, while some other studies showed that reduced extracellular pH together with higher intracellular pH could promote GC cell invasion and growth [43-45]. Here we preliminarily addressed whether intracellular alkalinization and reduced immunity are involved in downregulating PCAF levels in GC cells.

Although many genes have been analyzed to understand the molecular bases for human GC, only a few genes show frequent alterations [46-48]. Consistently, genetic alterations of PCAF, p16, and AE1 were not detectable in GC cells. As such, we propose that the aberrant loss of PCAF and storage of AE1 is associated with intracellular alkalinization and reduced IFN-γ secretion. Acidification of GC cells or IFN-γ treatment could induce PCAF expression that would eliminate the AE1-p16 interaction to reconnect the PCAF-p16-CDK4 pathway and eventually inhibit GC growth and improve GC patient prognosis. This possibility is consistent with information in public databases showing that elevated PCAF expression levels are associated with favorable prognosis and prolonged overall survival [30]. Hence, PCAF can be considered as a good marker for GC prognosis and may represent a novel treatment target.

Acknowledgements

This work was supported in part by the National Natural Science Foundation of China (No. 81-171939, No. 81372637, No. 81401956), the National Basic Research Program (973 Program, No. 2013CB910903), Key Projects in Shanghai Science & Technology Pillar Program for Biomedicine (No. 14431904700), and Shang-

hai Science and Technology Yang Fan Funds (No. 14YF1402300).

Disclosure of conflict of interest

None.

Abbreviations

PCAF, P300/CBP associating factor; GC, gastric cancer; AE1, anion exchanger 1; pHi, intracellular pH; PGC, poorly differentiated gastric cancer; WGC, well differentiated gastric cancer.

Address correspondence to: Dr. Guo-Hui Fu, Pathology Center, Shanghai General Hospital/Faculty of Basic Medicine, School of Medicine, Shanghai Jiao Tong University, No. 280, South Chong-Qing Road, Shanghai 200025, P. R. China. Tel: 86-21-63846-590-776601; E-mail: fuguhu@263.net

References

[1] Siegel RL, Miller KD and Jemal A. Cancer statistics, 2016. CA Cancer J Clin 2016; 66: 7-30.
[2] Lordick F and Janjigian YY. Clinical impact of tumour biology in the management of gastroesophageal cancer. Nat Rev Clin Oncol 2016; 13: 348-360.
[3] Shah MA. Gastrointestinal cancer: targeted therapies in gastric cancer-the dawn of a new era. Nat Rev Clin Oncol 2014; 11: 10-11.
[4] Van Cutsem E, Sagaert X, Topal B, Haustermans K and Prenen H. Gastric cancer. Lancet 2016; 388: 2654-2664.
[5] Chen Y, Guo ZQ, Shi CM, Zhou ZF, Ye YB and Chen Q. Efficacy of adjuvant chemotherapy combined with immunotherapy with cytokine-induced killer cells for gastric cancer after d2 gastrectomy. Int J Clin Exp Med 2015; 8: 7728-7736.
[6] Johnsson A, Durand-Dubief M, Xue-Franzen Y, Ronnerblad M, Ekwall K and Wright A. HAT-HDAC interplay modulates global histone H3K14 acetylation in gene-coding regions during stress. EMBO Rep 2009; 10: 1009-1014.
[7] Peserico A and Simone C. Physical and functional HAT/HDAC interplay regulates protein acetylation balance. J Biomed Biotechnol 2011; 2011: 371832.
[8] Verdin E and Ott M. 50 years of protein acetylation: from gene regulation to epigenetics, metabolism and beyond. Nat Rev Mol Cell Biol 2015; 16: 258-264.
[9] Fu M, Wang C, Zhang X and Pestell RG. Acetylation of nuclear receptors in cellular growth and apoptosis. Biochem Pharmacol 2004; 68: 1199-1208.
[10] Shiota M, Yokomizo A, Tada Y, Uchiumi T, Inokuchi J, Tatsugami K, Kuroiwa K, Yamamoto K, Seki N and Naito S. P300/CBP-associated factor regulates Y-box binding protein-1 expression and promotes cancer cell growth, cancer invasion and drug resistance. Cancer Sci 2010; 101: 1797-1806.
[11] Yoon H, Shin SH, Shin DH, Chun YS and Park JW. Differential roles of Sirt1 in HIF-1alpha and HIF-2alpha mediated hypoxic responses. Biochem Biophys Res Commun 2014; 444: 36-43.
[12] Simonsson M, Kanduri M, Gronroos E, Heldin CH and Ericsson J. The DNA binding activities of Smad2 and Smad3 are regulated by coactivator-mediated acetylation. J Biol Chem 2006; 281: 39870-39880.
[13] Patel JH, Du Y, Ard PG, Phillips C, Carella B, Chen CJ, Rakowski C, Chatterjee C, Lieberman PM, Lane WS, Blobel GA and McMahon SB. The c-MYC oncoprotein is a substrate of the acetyltransferases hGCN5/PCAF and TIP60. Mol Cell Biol 2004; 24: 10826-10834.
[14] Gaub P, Tedeschi A, Puttagunta R, Nguyen T, Schmandke A and Di Giovanni S. HDAC inhibition promotes neuronal outgrowth and counteracts growth cone collapse through CBP/p300 and P/CAF-dependent p53 acetylation. Cell Death Differ 2010; 17: 1392-1408.
[15] Kass EM, Poyurovsky MV, Zhu Y and Prives C. Mdm2 and PCAF increase Chk2 ubiquitination and degradation independently of their intrinsic E3 ligase activities. Cell Cycle 2009; 8: 430-437.
[16] Linares LK, Kiernan R, Triboulet R, Chable-Bessia C, Latreille D, Cuvier O, Lacroix M, Le Cam L, Coux O and Benkirane M. Intrinsic ubiquitination activity of PCAF controls the stability of the oncoprotein Hdm2. Nat Cell Biol 2007; 9: 331-338.
[17] Wan J, Zhan J, Li S, Ma J, Xu W, Liu C, Xue X, Xie Y, Fang W, Chin YE and Zhang H. PCAF-primed EZH2 acetylation regulates its stability and promotes lung adenocarcinoma progression. Nucleic Acids Res 2015; 43: 3591-3604.
[18] Malatesta M, Steinhauer C, Mohammad F, Pandey DP, Squatrito M and Helin K. Histone acetyltransferase PCAF is required for Hedgehog-Gli-dependent transcription and cancer cell proliferation. Cancer Res 2013; 73: 6323-6333.
[19] Gai X, Tu K, Li C, Lu Z, Roberts LR and Zheng X. Histone acetyltransferase PCAF accelerates apoptosis by repressing a GLI1/BCL2/BAX axis in hepatocellular carcinoma. Cell Death Dis 2015; 6: e1712.
[20] Kollmann K, Heller G, Schneckenleithner C, Warsch W, Scheicher R, Ott RG, Schafer M, Fajmann S, Schlederer M, Schiefer AI, Reichart U,

Mayerhofer M, Hoeller C, Zochbauer-Muller S, Kerjaschki D, Bock C, Kenner L, Hoefler G, Freissmuth M, Green AR, Moriggl R, Busslinger M, Malumbres M and Sexl V. A kinase-independent function of CDK6 links the cell cycle to tumor angiogenesis. Cancer Cell 2013; 24: 167-181.

[21] Rivadeneira DB, Mayhew CN, Thangavel C, Sotillo E, Reed CA, Grana X and Knudsen ES. Proliferative suppression by CDK4/6 inhibition: complex function of the retinoblastoma pathway in liver tissue and hepatoma cells. Gastroenterology 2010; 138: 1920-1930.

[22] Sherr CJ, Beach D and Shapiro GI. Targeting CDK4 and CDK6: from discovery to therapy. Cancer Discov 2016; 6: 353-367.

[23] von Witzleben A, Goerttler LT, Marienfeld R, Barth H, Lechel A, Mellert K, Bohm M, Kornmann M, Mayer-Steinacker R, von Baer A, Schultheiss M, Flanagan AM, Moller P, Bruderlein S and Barth TF. Preclinical characterization of novel chordoma cell systems and their targeting by pharmocological inhibitors of the CDK4/6 cell-cycle pathway. Cancer Res 2015; 75: 3823-3831.

[24] Liggett WH Jr and Sidransky D. Role of the p16 tumor suppressor gene in cancer. J Clin Oncol 1998; 16: 1197-1206.

[25] Liu Q, Song LJ, Xu WQ, Zhao L, Zheng L, Yan ZW and Fu GH. Expression of cytoplasmic p16 and anion exchanger 1 is associated with the invasion and absence of lymph metastasis in gastric carcinoma. Mol Med Rep 2009; 2: 169-174.

[26] Shen WW, Wu J, Cai L, Liu BY, Gao Y, Chen GQ and Fu GH. Expression of anion exchanger 1 sequestrates p16 in the cytoplasm in gastric and colonic adenocarcinoma. Neoplasia 2007; 9: 812-819.

[27] Rischin D, Young RJ, Fisher R, Fox SB, Le QT, Peters LJ, Solomon B, Choi J, O'Sullivan B, Kenny LM and McArthur GA. Prognostic significance of p16INK4A and human papillomavirus in patients with oropharyngeal cancer treated on TROG 02.02 phase III trial. J Clin Oncol 2010; 28: 4142-4148.

[28] Fu GH, Wang Y, Xi YH, Shen WW, Pan XY, Shen WZ, Jiang XS and Chen GQ. Direct interaction and cooperative role of tumor suppressor p16 with band 3 (AE1). FEBS Lett 2005; 579: 2105-2110.

[29] Kudrycki KE, Newman PR and Shull GE. cDNA cloning and tissue distribution of mRNAs for two proteins that are related to the band 3 Cl-/HCO3- exchanger. J Biol Chem 1990; 265: 462-471.

[30] Gyorffy B, Lanczky A, Eklund AC, Denkert C, Budczies J, Li Q and Szallasi Z. An online survival analysis tool to rapidly assess the effect of 22,277 genes on breast cancer prognosis using microarray data of 1,809 patients. Breast Cancer Res Treat 2010; 123: 725-731.

[31] Cui Y, Li SB, Peng XC, Wu J and Fu GH. Trastuzumab inhibits growth of HER2-negative gastric cancer cells through gastrin-initialized CCKBR signaling. Dig Dis Sci 2015; 60: 3631-3641.

[32] Tian H, Zhang N, Suo WH, Wang T, Song LJ, Wu J, Liu Q, Shen WW and Fu GH. Gastrin suppresses the interdependent expression of p16 and anion exchanger 1 favoring growth inhibition of gastric cancer cells. Int J Cancer 2010; 127: 1462-1474.

[33] Wang T, Zhao L, Yang Y, Tian H, Suo WH, Yan M and Fu GH. EGR1 is critical for gastrin-dependent upregulation of anion exchanger 2 in gastric cancer cells. FEBS J 2013; 280: 174-183.

[34] Wu J, Zhang YC, Suo WH, Liu XB, Shen WW, Tian H and Fu GH. Induction of anion exchanger-1 translation and its opposite roles in the carcinogenesis of gastric cancer cells and differentiation of K562 cells. Oncogene 2010; 29: 1987-1996.

[35] Patterson ST and Reithmeier RA. Cell surface rescue of kidney anion exchanger 1 mutants by disruption of chaperone interactions. J Biol Chem 2010; 285: 33423-33434.

[36] Wang T, Fei HJ, Yang Y, Jiang XS, Yan M, Zeng Z, Wu J, Song LJ, Tian H and Fu GH. Expression of AE1/p16 promoted degradation of AE2 in gastric cancer cells. BMC Cancer 2016; 16: 716.

[37] Suo WH, Zhang N, Wu PP, Zhao L, Song LJ, Shen WW, Zheng L, Tao J, Long XD and Fu GH. Anti-tumour effects of small interfering RNA targeting anion exchanger 1 in experimental gastric cancer. Br J Pharmacol 2012; 165: 135-147.

[38] Li Q, Liu Z, Xu M, Xue Y, Yao B, Dou C, Jia Y, Wang Y, Tu K, Zheng X and Yao Y. PCAF inhibits hepatocellular carcinoma metastasis by inhibition of epithelial-mesenchymal transition by targeting Gli-1. Cancer Lett 2016; 375: 190-198.

[39] Stimson L, Rowlands MG, Newbatt YM, Smith NF, Raynaud FI, Rogers P, Bavetsias V, Gorsuch S, Jarman M, Bannister A, Kouzarides T, McDonald E, Workman P and Aherne GW. Isothiazolones as inhibitors of PCAF and p300 histone acetyltransferase activity. Mol Cancer Ther 2005; 4: 1521-1532.

[40] Eck M, Schmausser B, Scheller K, Brandlein S and Muller-Hermelink HK. Pleiotropic effects of CXC chemokines in gastric carcinoma: differences in CXCL8 and CXCL1 expression between diffuse and intestinal types of gastric carcinoma. Clin Exp Immunol 2003; 134: 508-515.

[41] Devi S, Ansari SA, Vadivelu J, Megraud F, Tenguria S and Ahmed N. Helicobacter pylori antigen HP0986 (TieA) interacts with cultured gastric epithelial cells and induces IL8 secretion via NF-kappaB mediated pathway. Helicobacter 2014; 19: 26-36.

[42] Zhao YH, Wang T, Yu GF, Zhuang DM, Zhang Z, Zhang HX, Zhao DP and Yu AL. Anti-proliferation effects of interferon-gamma on gastric cancer cells. Asian Pac J Cancer Prev 2013; 14: 5513-5518.

[43] Chen M, Zou X, Luo H, Cao J, Zhang X, Zhang B and Liu W. Effects and mechanisms of proton pump inhibitors as a novel chemosensitizer on human gastric adenocarcinoma (SGC7901) cells. Cell Biol Int 2009; 33: 1008-1019.

[44] Yeo M, Kim DK, Kim YB, Oh TY, Lee JE, Cho SW, Kim HC and Hahm KB. Selective induction of apoptosis with proton pump inhibitor in gastric cancer cells. Clin Cancer Res 2004; 10: 8687-8696.

[45] Zhao W, Lu M and Zhang Q. Chloride intracellular channel 1 regulates migration and invasion in gastric cancer by triggering the ROS-mediated p38 MAPK signaling pathway. Mol Med Rep 2016; 13: 3711.

[46] Guilford P, Hopkins J, Harraway J, McLeod M, McLeod N, Harawira P, Taite H, Scoular R, Miller A and Reeve AE. E-cadherin germline mutations in familial gastric cancer. Nature 1998; 392: 402-405.

[47] Uchino S, Tsuda H, Noguchi M, Yokota J, Terada M, Saito T, Kobayashi M, Sugimura T and Hirohashi S. Frequent loss of heterozygosity at the DCC locus in gastric cancer. Cancer Res 1992; 52: 3099-3102.

[48] Yamada Y, Yoshida T, Hayashi K, Sekiya T, Yokota J, Hirohashi S, Nakatani K, Nakano H, Sugimura T and Terada M. p53 gene mutations in gastric cancer metastases and in gastric cancer cell lines derived from metastases. Cancer Res 1991; 51: 5800-5805.

Supplementary Table 1. Lower expression of PCAF was correlated with poor differentiation

Clinicopathological feature	Total	PCAF Positive rate (%)	PCAF Weak positive rate (%)	PCAF Negtive rate (%)	*p* value
Grade	210				0.000
G1	97	0.76	0.22	0.02	
G2	88	0.43	0.45	0.11	
G3	25	0.12	0.56	0.32	
Gender	204				0.578
Male	139	0.55	0.37	0.09	
Female	65	0.57	0.31	0.12	
Age (year)	195				0.082
≤60	114	0.61	0.32	0.08	
>60	81	0.44	0.43	0.12	
Lump size	190				0.617
≤4	117	0.57	0.34	0.09	
>4	73	0.52	0.41	0.07	
Lymph metastasis	211				0.222
Negtive	69	0.52	0.33	0.14	
Positive	142	0.56	0.37	0.07	
Blood vesselsmetastasis	210				0.111
Negtive	201	0.56	0.35	0.09	
Positive	9	0.22	0.56	0.22	
Lauren classification	215				0.007
Intestinal type	84	0.54	0.31	0.15	
Diffuse type	110	0.57	0.36	0.06	
Mixed type	21	0.33	0.67	0.00	
TNM staging	210				0.291
0	9	0.67	0.22	0.11	
1	36	0.36	0.47	0.17	
2	71	0.58	0.31	0.11	
3	91	0.58	0.36	0.05	
4	3	0.67	0.33	0.00	
Depth of invasion	201				0.292
T1	15	0.47	0.40	0.13	
T2	40	0.45	0.40	0.15	
T3	97	0.57	0.33	0.10	
T4	49	0.59	0.39	0.02	